2

CONF-8905134--2

UCRL- 101020
PREPRINT

Received by OSTI

JUN 0 9 1989

COMPUTER EXPERIMENTS ON LP JET INJECTION STABILITY AND INCIPIENT BREAKUP

Alfred C. Buckingham

This is a preprint of a paper to be presented and published as part of the Proceedings of the 1989 JANNAF Propulsion Meeting, to be held at the NASA Lewis Research Center, Cleveland, Ohio, May 22-25, 1989

April 1989

Lawrence Livermore National Laboratory

This is a preprint of a paper intended for publication in a journal or proceedings. Since changes may be made before publication, this preprint is made available with the understanding that it will not be cited or reproduced without the permission of the author.

DISCLAIMER

This report was prepared as an account of work sponsored by an agency of the United States Government. Neither the United States Government nor any agency thereof, nor any of their employees, makes any warranty, express or implied, or assumes any legal liability or responsibility for the accuracy, completeness, or usefulness of any information, apparatus, product, or process disclosed, or represents that its use would not infringe privately owned rights. Reference herein to any specific commercial product, process, or service by trade name, trademark, manufacturer, or otherwise does not necessarily constitute or imply its endorsement, recommendation, or favoring by the United States Government or any agency thereof. The views and opinions of authors expressed herein do not necessarily state or reflect those of the United States Government or any agency thereof.

MA

DISTRIBUTION OF THIS DOCUMENT IS UNLIMITED

DISCLAIMER

This report was prepared as an account of work sponsored by an agency of the United States Government. Neither the United States Government nor any agency thereof, nor any of their employees, makes any warranty, express or implied, or assumes any legal liability or responsibility for the accuracy, completeness, or usefulness of any information, apparatus, product, or process disclosed, or represents that its use would not infringe privately owned rights. Reference herein to any specific commercial product, process, or service by trade name, trademark, manufacturer, or otherwise does not necessarily constitute or imply its endorsement, recommendation, or favoring by the United States Government or any agency thereof. The views and opinions of authors expressed herein do not necessarily state or reflect those of the United States Government or any agency thereof.

DISCLAIMER

Portions of this document may be illegible in electronic image products. Images are produced from the best available original document.

COMPUTER EXPERIMENTS ON LP JET INJECTION STABILITY AND INCIPIENT BREAKUP*

A.C. Buckingham
Center for Compressible Turbulence
UNIVERSITY OF CALIFORNIA
LAWRENCE LIVERMORE NATIONAL LABORATORY
Livermore, California 94550

UCRL--101020

DE89 012967

T.P. Coffee
Interior Ballistics Modeling Branch
BALLISTICS RESEARCH LABORATORY
Aberdeen Proving Ground, Maryland 21005-5066

ABSTRACT

A hybrid Lagrangian (computational mesh moving with the center of mass of the fluid element) Eulerian (stationary, laboratory-frame computational mesh) fast Fourier transform (FFT) procedure and a continuously rezoned Lagrangian-Eulerian finite-difference procedure are modified here for study and analysis of LP jet injection dynamics. Specific attention is on development, test, and application of computer models which will predict influences of chamber pressure, jet-injection velocity and combustion energy release on the LP jet injection-flow configuration. The injection flow changes of particular interest are those which might signify tendencies for either jet stream segmentation and breakup or intact jet stream penetration of the entire combustion chamber in LP gun propulsion. Information also is sought on fuel segment size distribution following jet stream breakup, and the steady-state or oscillatory parameter changes that seem to most influence LP fuel segmentation. The initial studies emphasize the role of flow instabilities in forming or suppressing fuel-stream breakup and, perhaps, influencing subsequent segment or droplet-size distribution tendencies. Attention is focused, at present, on the primary Rayleigh-Taylor density penetration instability growth and secondary Kelvin-Helmholtz shear instability growth patterns. Response to naturally developed or forced, narrow-band oscillatory changes in the more influential parameters will be analyzed subsequently.

INTRODUCTION

THE CONCEPT

The jet stream is considered to sustain an initial space and time distribution of single wave, multiple wave, or random small disturbances. Small disturbances here refer to imposed radial-velocity component perturbations in

*This is a report of work performed under the auspices of the U.S. Department of Energy by the Lawrence Livermore National Laboratory under Contract No. W-7405-Eng-48 and supported, in part, by a joint Department of Energy, Department of Defense Memorandum of Agreement through the U.S. Army Ballistic Research Laboratory, Aberdeen Proving Ground MD.

which the product of wave length times frequency is less than or equal to 1% of the mean jet streaming velocity. Both jet leading-edge Rayleigh-Taylor (vapor-liquid interpenetration) and jet side Kelvin-Helmholtz (vapor-liquid interface shear) instabilities are presumed primary sources of the tendency of the jet stream to corrugate, form extended tendrils, and ultimately to break into droplets.

Previous numerical simulation results emphasized the role of pressure oscillations on the breakup of thin injected liquid-fuel sheets. The primary role of the Rayleigh-Taylor instability mode on ligand and surface-wave formation following deceleration of the jet leading edge in an oscillating pressure field was the focus of these previous studies.(1,2) Simulation results indicated the probability that nonlinear combinations of Rayleigh-Taylor, Kelvin-Helmholtz and, perhaps, other distinctly identifiable primary or secondary instability modes are active in liquid jet sheet breakup. In contrast, injection pressure, chamber pressure , jet velocity and jet liquid material properties, such as surface tension and viscosity, may act either to promote or suppress the instability growth. Hence, this may affect the time required for initiating jet breakup and the size of the incipient jet breakup segments that are formed.

The primary interest in this modeling effort is to develop a reasonably accurate technique for estimating jet breakup times under various jet injection and combustion chamber background conditions. Of equal interest is obtaining predictive capability for estimating droplet-size distributions once breakup has occurred. The basic notion is that we may be able to obtain breakup time estimates and discontinuous fuel-segment size scales by tracing interface instability growth scales until severe contractions in the continuous jet-fluid film thickness has occurred. Criteria for breakup may subsequently be included in the predictions based on the conditional information obtained from the numerical simulations and the material properties of the fluid. We will discuss results of some preliminary computations to illustrate the procedure, subsequently. At present, it will be useful to review some information on liquid jet-injection dynamics, breakup tendencies, and what we feel are pertinent results on liquid-vapor instability studies.

LP JET FUEL INJECTION

Ideally, an injected jet stream of LP breaks up almost immediately into an almost uniform dispersal of small-diameter (tens of microns mean diameter) droplets. This idealized droplet spray pattern diverges rapidly into the high pressure, high temperature combustion chamber where the ensemble of small fuel droplets vaporize and ignite. This ideal small-droplet spray combustion picture is thermodynamically efficient since the surface area-to-volume ratio of the droplets promotes complete consumption of the fuel with little liquid residue remaining for deposition on chamber walls or within the gun tube, itself.

Unfortunately, this small-droplet spray combustion picture remains only an idealization. It is not commonly realized in practical high pressure combustion applications. In a recent review, Bracco (3) remarks about the lack of

experimental information on jet stream dynamics and breakup at the high pressures (O 20 MPa or greater) and high temperatures (O 2700 K or greater) encountered in LP gun combustion. Additional difficulties develop from the sizeable pressure permutations about the mean chamber pressures (± 50%) that may occur. The oscillating-pressure time histories, sometimes realized, may occur at critical jet formation eigenfrequencies.

Bracco (3) also points out that the lack of fundamental measurements of LP thermodynamic, transport, and constitutive properties at LP gun conditions may prevent obtaining anything but qualitative information and implications when analyzing and modeling these situations. We suggest, however, that two-dimensional calculations may provide useful insight in identifying the influence of jet inlet to combustion-chamber geometry on fuel-stream segmentation and cavitation and, perhaps, with simplifying assumptions on boundary conditions, and the effect of swirl on promoting small-droplet formation and dispersion.

It is clear also that the parametric influences of permuted changes to unknown property values may be explored for sensitivity about some mean, reasonable, values adopted even in the absence of measured property data. For example, we have and will use computer simulations to examine the influence of imposed oscillatory pressure influences at theoretically identified critical eigenfrequencies for jet-pattern changes and jet-stream breakup.

The present work exemplifies this use of computer simulations. We focus on cold flows, emphasizing the fluidynamic aspects. This paper will discuss Rayleigh-Taylor instabilities, which will be generated at the leading edge of the injected liquid. In a later paper we will discuss Kelvin-Helmholtz instabilities, which will be generated along the sides of the injected liquid. We reserve for later analysis the undoubtedly significant influence of combustion energy release, rate, and time history on the injection dynamics.

RELATED INSTABILITIES

To provide some perspective on the changes to flow configurations that may signal the onset of jet breakup and fuel droplet or large fuel clump (non-atomization) formation, we review some non-affine, but dynamically-related multifluid instability-generated interpenetration, breakup, and mixing investigations.

In a definitive set of rocket-sled accelerated, stratified density fluid mixing experiments, numerical simulations, and analyses, Youngs (4) and Read (5) identified the influence of superimposed fluid layer material density, ρ_1, ρ_2, velocity, $\vec{q}$, and acceleration $\dot{\vec{q}}$ on material interface instability evolution, consequent material interpenetration, breakup and macroscopic scale (clump/droplet) mixing. Here, the indices (1) and (2) refer to the two distinct fluids which may possess densities very different (say, normal vapor vs normal liquid),

$$A_T \rightarrow 1.0\,, \tag{1a}$$

or almost identical (say the incompressible limit for two layers of the same fluid)

$$A_T \rightarrow 0\,. \tag{1b}$$

Here A_T is the reduced interface-density difference or, as it is better known, the Atwood Number. This parameter is used to categorize multidensity material interface mixing processes such as in jets or free-shear layers,

$$A_T \equiv \frac{|\rho_1 - \rho_2|}{\rho_1 + \rho_2} \tag{1c}$$

In the Youngs-Read investigations, $\vec{q}$, is vector aligned with the local gravitational acceleration, $\vec{g}$. Constant acceleration, from an impulsive start, is given to an optically transparent container. Phases of interface instability growth, interpenetration, breakup, material size-scale distributions, and mixing are explicitly traced using rapid exposure optical shadowgraph diagnostics in association with a fast-framing camera.

Two-dimensional (laterally broad) and three-dimensional (laterally narrow) channel configurations were dynamically tested. Both primary Rayleigh-Taylor and secondary Kelvin-Helmholtz instabilities were found to be influentially active at different (not necessarily coincident) stages in the fluid interface breakup and mixing. Dynamic, if not geometrically affine similarities exist, with respect to LP jet instability, interpenetration, breakup, entrainment and mixing of two fluids. Limiting growth stages are identified as useful benchmarks in defining phases of material-interface instability breakup and mix experiments and analyses. As an example, let us define the temporally growing amplitude of an instability, a(t), at the initiation of a Rayleigh-Taylor (interpenetration) acceleration-driven instability,

$$a\,(t) = a_0 \exp\,(N_\lambda t)\,, \tag{2}$$

in terms of its initial (linear) growth rate, N_λ,

$$N_\lambda^2 = \vec{k}\dot{\vec{q}}A_T, \tag{3a}$$

where $\vec{k}$ is the vector wave number associated with a principal wave length, λ^*, advected with the fluid velocity, $\vec{q}$. In terms of this wave length, (3a) often is expressed

$$N_\lambda^2 = \frac{2\pi}{\lambda^*}\dot{\vec{q}}A_T\,. \tag{3b}$$

Selectively in the linear range, the smallest wave length perturbation is seen from (3b) to grow the most rapidly, outrunning all other wave lengths, at least in the absence of viscosity.

The primary effect of viscosity may be deduced from Chandresekhar's [6] definitive small perturbation analysis of the Kelvin-Helmholtz shear instability growth rate. For two fluid layers with densities ρ_1, and ρ_2, assume existence of uniform invariant dynamic viscosity coefficients μ_1 and μ_2. Under this constraint on material homogeneity, an effective kinematic viscosity is defined,

$$\bar{\nu} = \frac{\mu_1 + \mu_2}{\rho_1 + \rho_2} . \tag{4}$$

Now, in a real viscous two-fluid mixing layer, the principal wave length, λ^* of Eqn (3b) is no longer arbitrary but is determined by the average interface viscosity. It is identified as the <u>most</u> <u>unstable</u> wave length

$$\lambda^* = \lambda_M = 4\pi \left\{ \frac{\bar{\nu}^2}{\dot{\vec{q}}} \left(A_T^{-1} \right) \right\}^{1/3} \tag{5}$$

and N_λ is replaced by the maximum initial growth rate in a viscous fluid,

$$N_\lambda \equiv N_M = \left\{ \frac{\pi \dot{\vec{q}}}{\lambda_M} A_T \right\}^{1/2} . \tag{6}$$

This first stage of instability growth signals the initial onset of filamentary wave growth in the fuel sheet. This stage lasts until the amplitude, a(t) becomes the same <u>order</u> as the most unstable wave length, λ_M.

A second stage of instability growth now appears in which <u>larger</u> wave lengths <u>grow</u> <u>more</u> <u>rapidly</u> than smaller ones. The less dense fluid penetrates the more dense with a fixed "bubble" growth velocity given according to Youngs' and Read's results by [4,5]

$$v_\perp^b = C_1^* \sqrt{\dot{\vec{q}} \lambda} \tag{7}$$

where the constant, C_1, is empirically determined as $0.15 \leq C_1 \leq 0.3$.

An earlier, independent theoretical study by Layzer [7] based on a singular perturbation analysis has been expanded recently to third order where the relatively weak compressibility influence first emerges. This may indicate that the observations about the second-phase growth, favoring the larger wave lengths, may be a valid benchmark for estimating onset to interface breakup in the combustion (energy release) analyses which are planned subsequent to

these cord flow investigations. In particular, Layzer's results show, at this intermediate stage, the limiting vapor (less dense) penetration velocity tends to

$$v_{\perp}^{b} = \left(\frac{\dot{\vec{q}}\lambda}{6\pi}\right)^{1/2} \simeq 0.23\sqrt{\dot{\vec{q}}\lambda} \tag{8}$$

This compares favorably with Eqn (7) when in a two-dimensional gravitational, $\vec{g}$, field. In three dimensions, Layzer's theoretical results predict that this limiting vapor penetration velocity increases slightly to

$$v_{\perp}^{b} = \left(\frac{\dot{\vec{q}}\lambda}{2\beta_1}\right)^{1/2} \simeq 0.36\sqrt{\dot{\vec{q}}\lambda}\,, \tag{9}$$

where β_1 is the first zero of Bessel Function J_0.

As reinforced by Youngs' and Read's investigations, this phase extends until the dominant amplitude $a_d(t)$ has grown to about 10 λ_M, at which time the linear modes are saturated and nonlinear growth sets in.

DISCUSSION

SCALES

We note from our previous instability review, that the second-phase growth velocity introduces a length scale, λ, independent of or in contrast with the minimum length scale λ^* or λ_M of the first phase, Eqs 3b and 6. Moreover, this growth at a later stage favors the larger, as opposed to the smaller, length scales. The independence of the intermediate instability growth and the characteristic scale of the flow instability structures, which may separate into clumps or droplets, is independent at an intermediate stage with respect to the initial stage. Memory of initial conditions, thereby, is lost at an intermediate time.

In the last stage, an average similarity growth associated with development of a random, turbulent inter-mixing field, is apparent. For scale widths $\approx 10\lambda_M$, there emerges a characteristic single large scale, identified as the two-fluid interpenetration range or "mixing" length,

$$\delta_M = A^*F(\rho_1/\rho_2)\vec{g}t^2 = A^*F\ (\rho_1/\rho_2)\dot{\vec{q}}t^2\,, \tag{10}$$

where F is a density ratio-dependent similarity variable and A^* is a constant. For the dense-fluid penetration studies of Youngs and Read [4,5], $F(\rho_1/\rho_2) = A_T$

and $.04 \leq A^* \leq .05$, dense fluid, 2-D geometry
and (11)
$.063 \leq A^* \leq .077$, dense fluid, 3-D geometry,

from these empirical observations, one may conclude that the 2-D constraints are more suppressive of growth degrees of freedom than are the 3D.

In the foregoing, we have summarized some growth rates and developed characteristic length scales that may be useful for estimation of ultimate fluid segment or droplet size following breakup of the jet. These estimates may be useful as "benchmarks" for evaluating the accuracy and progress of a numerical simulation as it approaches characteristic limiting values (length and time). The numerical results may, in turn, be applied to estimate macroscopic dimensions of discontinuous fluid entities and their initial dispersal.

Other indications are that modest compressibility influences (for the subsequent energy release investigations) also may be estimated. For example, we may identify these influences by applying the asymptotic estimates, Eqs (8) and (9), at intermediate stages of jet breakup segmentation or with reference to Chandrasekhar [6] and the stratified density analyses of Plesset and Hsieh [8], one may obtain the compressibility corrections of the basic linear growth rate, N_0, of the form:

$$N_c^2 = N_0^2\left[1 + \frac{\rho_1 \rho_2}{(\rho_1 + \rho_2)^2}\left(\frac{v^2}{a_2^2} - \frac{v^2}{a_1^2}\right)\right] \tag{12}$$

Here a_1 and a_2 are the acoustic (sound speeds) in fluids (1) and (2), respectively, and v is the surface wave velocity.

PROCEDURE

All calculations in this paper were done using the LAMPS code. This hybrid Euler-Lagrange pseudo-spectral procedure was modified and reconfigured for analysis of impulsively accelerated Rayleigh-Taylor instabilities in real viscous two-fluid computations of liquid propellant combustion instabilities. [1,2]

The Lagrangian phase of the pseudospectral hybrid Lagrange-Euler calculation includes a discretized time-advancement (evolutionary) step. This effectively traces the discrete motions of a prescribed number of material boundaries, b_i, in a cartesian x-y space. A stationary Eulerian mesh projects in physical space as equally discretized spanwise points over which the Lagrange material lines move in discrete time increments. The spanwise velocity, associated flux quantities and derivatives are evaluated by expanding in a truncated Fourier series

$$\Phi(x) = \sum_{k=k^*}^{k^*} \Phi_k \exp(ikx), \tag{13}$$

at each discrete time interval, $t_j = t_0 + N_j\Delta t$. In Eq. (14), $\Phi(k)$ is a dependent variable which is 2π periodic in the range, $x \subset [0., xmax]$. The integer wave number is represented by k and truncation is at $|k| \equiv k^*$. The Fourier spectral coefficient is represented by Φ_k To avoid high wave number aliasing errors from products evaluated in the phase plane, we use a collocation scheme containing 3k evenly spaced spanwise, x, points in the physical plane. Transforms between phase plane and configuration space take place at each explicit timestep. Derivatives are evaluated in phase space. The nonlinear (velocity product) terms are evaluated in configuration space.

Let u represent the transverse component of the fluid velocity, v the y-component of the b_i line velocity, and V is the material y-component of velocity,

$$V = v + \left(\frac{\partial y}{\partial x}\right)\Big|_b \; u \equiv v + \left(\frac{\partial b/\partial x}{\partial b/\partial y}\right) u \,. \tag{14}$$

In our formulation p is the scalar pressure, ρ is the mass density and I the internal density of the fluid per unit volume. The v component is solved as a kinematic condition on the y motion of the b_i interfaces whose instantaneous position yields two metrics. These relate the interface compressibility and slope, respectively, in an x,y cartesian space,

$$\begin{aligned} \alpha(x, b_i, t) &\equiv \frac{\partial y}{\partial b}\Big|_x \,, \\ \beta(x, b_i, t) &\equiv \frac{\partial y}{\partial x}\Big|_b \,. \end{aligned} \tag{15}$$

The governing system of transformed differential equations relate the fixed cartesian (x,y,t) plane and the kinematic (x, b_i, t) plane. The resulting time-evolution or "tendency" equations are:

$$\frac{\partial u}{\partial t} = \frac{-\partial(\mu u)}{\partial x} \,, \tag{16}$$

$$\frac{\partial(\mu u)}{\partial t} = \frac{\partial(\beta p)}{\partial b} - \frac{\partial(\alpha p)}{\partial x} - \frac{\partial(\mu u^2)}{\partial x} \tag{17}$$

$$\frac{\partial(\mu V)}{\partial t} = \frac{\partial p}{\partial b} - \frac{\partial(\mu u V)}{\partial x} \,, \tag{18}$$

$$\frac{\partial(\mu e)}{\partial t} = -p\left\{\frac{\partial(\alpha u)}{\partial x} + \frac{\partial v}{\partial b} - \frac{\partial \beta u}{\partial b}\right\} - \frac{\partial(\mu u e)}{\partial x} \tag{19}$$

$$\frac{\partial y}{\partial t} = v \,. \tag{20}$$

Where we introduce, for convenience, $\mu = \alpha p$ and $e \equiv 1/\rho$ .. Numerical time integration of the tendency equations, Eqs 16-20, is approximated using a conventional third-order Runge Kutta procedure, together with an equilibrium equation of state expressing thermodynamic closure,

$$p = p(\rho, e) \,. \tag{21}$$

Periodicity in boundary conditions and planar (infinite radius of curvature) assumptions on principal wave number of the Fourier expansions limit the spectral collocation code applications to the thin-film sheet jet injection modeling of Rayleigh-Taylor and secondary Kelvin-Helmholtz interactions, Fig. 1. We use this code and configuration to examine vibrational eigenvalues and their influence on wave length and amplitude of jet leading edge instabilities.

The SHALE Lagrange-Euler continuous rezoning case is used to simulate the axial symmetry of annular LP injection geometry. For example, Fig. 2 shows one such prototype regenerative injection system with a dynamically driven variable area throat designed to help control combustion chamber pressure oscillations. The SHALE code originated at Los Alamos

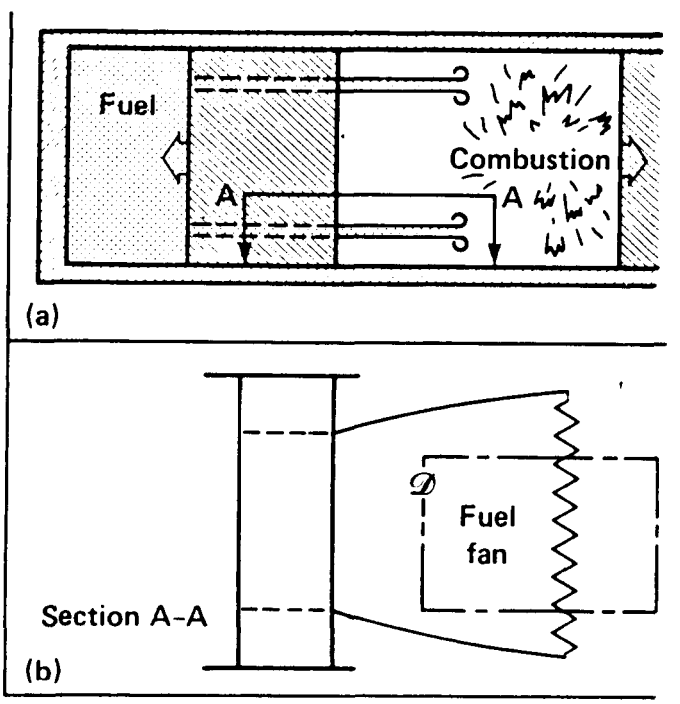

Figure 1. Representation of fuel fan domain, $\mathfrak{D}$, considered as a representation of a thin, flat, two-dimensional jet sheet.

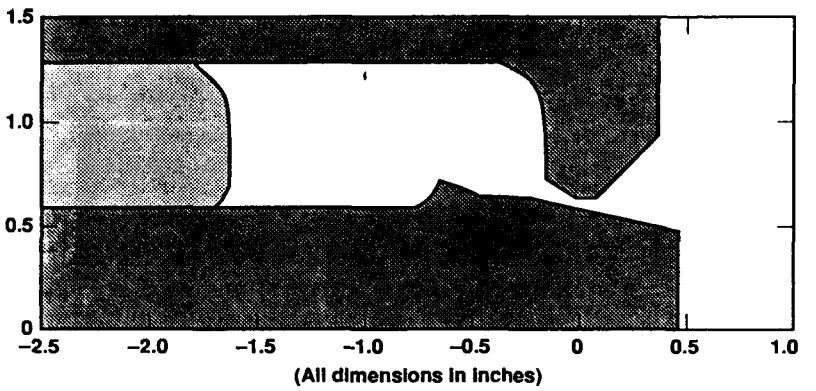

Figure 2. Sketch of a prototype regenerative LP nozzle with dynamically variable throat area which issues a thin axisymmetric annular jet of LP. The 0. axis is the rotational generator axis of symmetry for the cylindrical nozzle.

as a geophysical material modification of the well known "ICE-ALE" (implicit-compressible-explicit, arbitrary Lagrange-Euler mesh) procedure. A later, Livermore-developed [11,12] fluid version is being modified to simulate axisymmetric, viscous LP jet injection flow. Results of the SHALE code simulations will be given in a future paper.

INITIAL RESULTS

In the introduction, the temporal evolution of primary Rayleigh-Taylor penetration and secondary Kelvin-Helmholtz shear instabilities for interpenetrating fluids of different densities were traced through three distinct stages. Two of these stages, or growth phases, were linear (initial and intermediate growth phases) and one nonlinear (late time coasting evolution) vapor penetration and cavitation onset. Limiting length scales and their growth rate, as discussed previously, are uniquely defined in each phase. Small-scale initial dominance was shown replaced by dominance of the largest scales in the intermediate phase. Memory of initial conditions is lost at the intermediate stage. In the third, nonlinear growth phase, the characteristic length scale for vapor penetration in liquid density was introduced and verified with respect to experimental observations [4,5] and asymptotic analysis [6,7,8].

In addition, we described prescriptions for predicting/correcting for the influence of compressibility (heat release), viscosity, and surface tension on the growth rate and scale (size) dimensions of the instability structures. Where possible, we have and will supplement the results of classical perturbation instability analysis with interpretations of contemporary observations that show promise in predicting droplet or clump size and dispersal as a function of jet properties, geometry and flow conditions. [10,4,5] The code simulations are also useful for testing sensitivity of changes to injection design conditions and injected flow material properties and to suggest system changes that show promising characteristics for later experimental test and verification.

From our earlier results, we may review the influence of pressure oscillations on thin, injected fuel sheets. They directly influence amplitude and wave length reduction of jet injection sheet instabilities and the subsequent spread of the combustion vapor, fuel sheet interpenetration zone. The spectral transform collocation procedure [1,2] results seen in Fig. 3 illustrate that the principal leading edge jet penetration Rayleigh-Taylor growth rate, by and large, satisfactorily follows that predicted by theory the late times. Our interest here is on the effect of applying oscillatory pressure excitation at the first resonance steady-state injection fuel sheet oscillation.

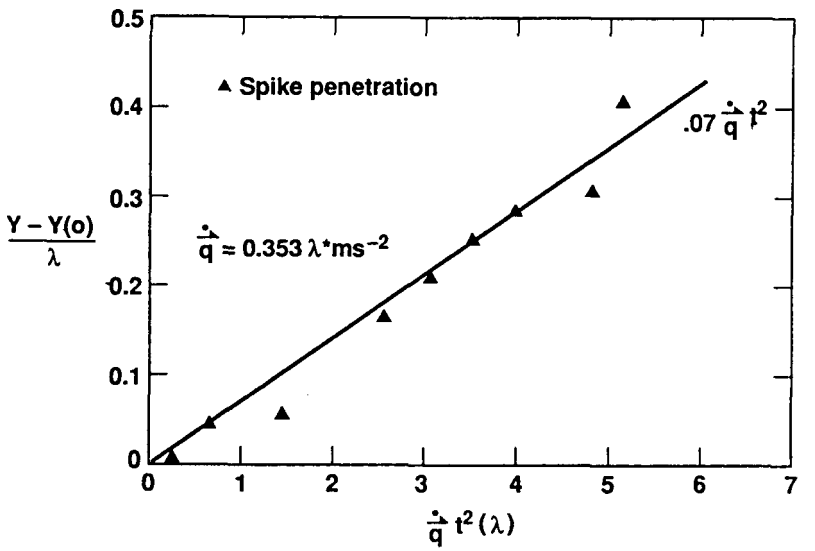

Figure 3. Instability growth as a function of the product of mean acceleration and square of the flow time for uniform acceleration.

The results in Figs. 4 and 5 illustrate that fuel-to-vapor penetration rate is reduced as are the wave length and scale of the leading edge jet fan perturbations. The implications are that the characteristic size of the segments or droplets could also be reduced by narrow-band forced vibrations. Note, particularly in Fig. 5 that both amplitude and wave length of the larger scale liquid interface undulations may be reduced by introduction of critical eigenfrequency pressure oscillations.

Next, the numerical simulations provide an illustration of the influence of variations in injection jet velocity and, consistently, the injection to combustion chamber pressure drop. The injection jet velocity and its influence on retarding jet injection breakup and segmentation are of primary interest in this stage of analysis. Specifically, consider the influence of $\overline{U}_o \pm \Delta U$ where $\overline{U}_o$ is the mean injection velocity and $|\Delta U|$ is the incremental velocity change, $U^{*}-\overline{U}_o$ imposed by a change in pressure drop for physical realizability. These results were obtained using the pseudospectral code examining permutations to the longitudinal (streaming) velocity (parallel to the injection path). The mean

velocity is nominally 150 m/s. Case A corresponds to a 1.6 MPa baseline pressure drop while Case H is permuted to a value of 6.7 MPa pressure drop.

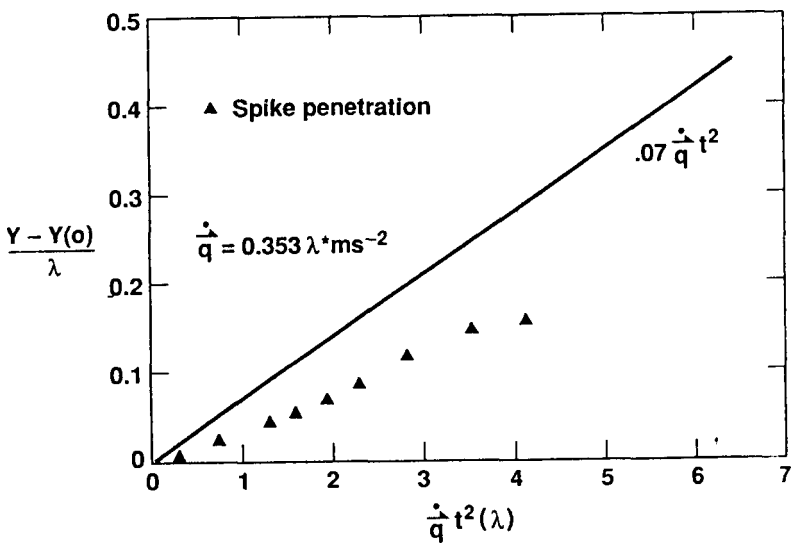

Figure 4. Instability growth as a function of the product of mean acceleration and square of the flow time for pressure oscillation induced-perturbations about an otherwise uniform acceleration.

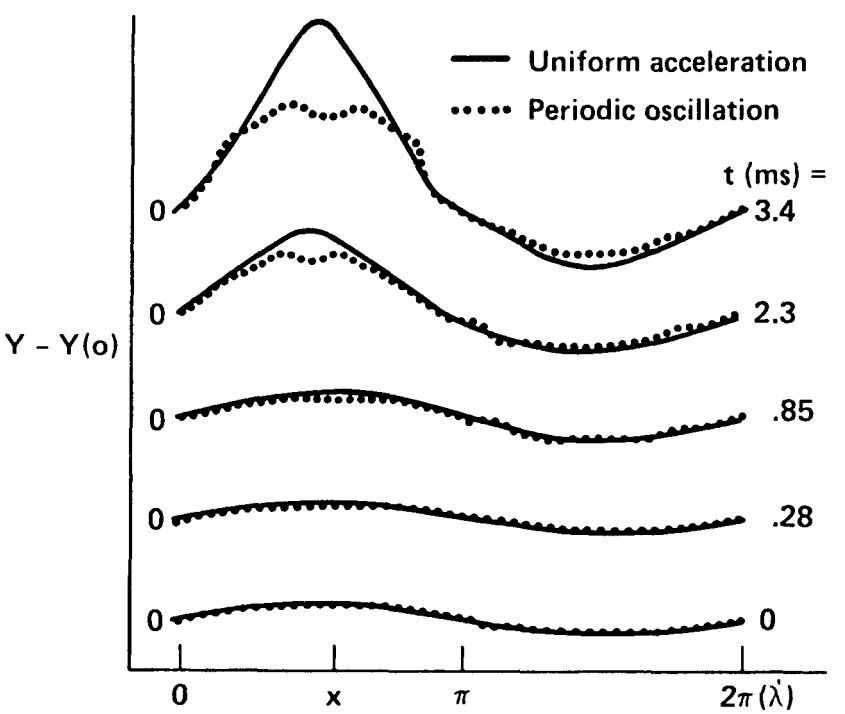

Figure 5. Alterations by applied pressure oscillations to Rayleigh-Taylor interface instability fuel jet leading edge decelerating into high pressure vapor.

Figure 6 shows the incremental (permuted) change in mean jet velocity resulting from prescribed boundary conditions on pressure-drop changes as a modest percentage of the mean value supporting $\overline{U}_o$. The programmed changes to injection velocity, U*, develop as a function of instantaneous change to the mean pressure drop rather than changes to the injection velocity itself. The velocity time histories become physically realizable. Figure 6 displays the changes to the injection velocity ratioed to the mean as a function of time. The purposely physically realizable changes to jet velocity lag step function pressure drop changes by a small-phase increment, seen in Fig. 6.

The velocity lag is that associated with the inertia of the flow which adjusts itself to the prescribed change in pressure accelerating the flow realistically, yet simply, to a new velocity over a finite-time interval. The tests on this segment of flat fuel fan are, in effect, terminated by the finite range of the segment (and the calculation) by a boundary limitation on signal-path propagation (and reflected error) at or about a dimensionless time of 3.

This dimensionless time is related to the wave number increment Δ_k used for the Fourier-basis function expansions in this test. That is for wave number increment

$$\Delta k_o = \pi/12\lambda ,$$

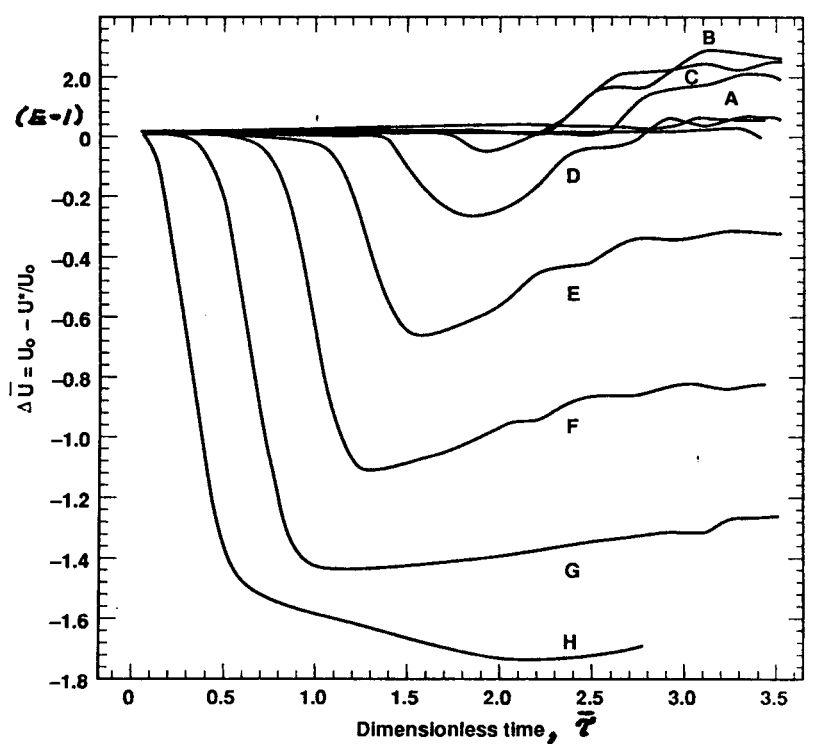

Figure 6. Jet injection velocity changes induced by permutations to the baseline pressure drop in pseudospectral jet sheet injection simulations.

where λ is the streamwise extent of the domain, the dimensionless time is given by

$$\bar{\tau} = t/\tau_o \text{, where t is physical time and}$$

$$\tau_o \equiv (\Delta k_o u_o)^{-1} .$$

Velocity permutations in Fig. 6 are identified by letter. The largest change, about 17% increase over the mean velocity is labeled "H". The maximum decrease in velocity, labeled about 3%, corresponds to the letter "B".

The resulting instability deformations to the fuel-vapor interface are plotted as percentages of the fuel-sheet thickness, Δ for sample streamwise velocity changes G, D, and B. These show the influence of the second highest intermediate and lowest increases about the mean velocity, respectively. The highest value, H, was not included since the boundary influences shortened the constant velocity period inconveniently for comparative analysis. Figure 7 shows maximum sheet deformations reaching about 10% of the original thickness at $\tau = 1.50$. Figure 8 shows deformations approaching 40% of the thickness at $\tau = 2.50$.

The largest permutations in streaming velocity are seen to effectively create the largest suppression of the influence of the original leading edge Rayleigh-Taylor instability as it moves over the liquid-propellant sheet as a propagating wave toward the injection nozzle.

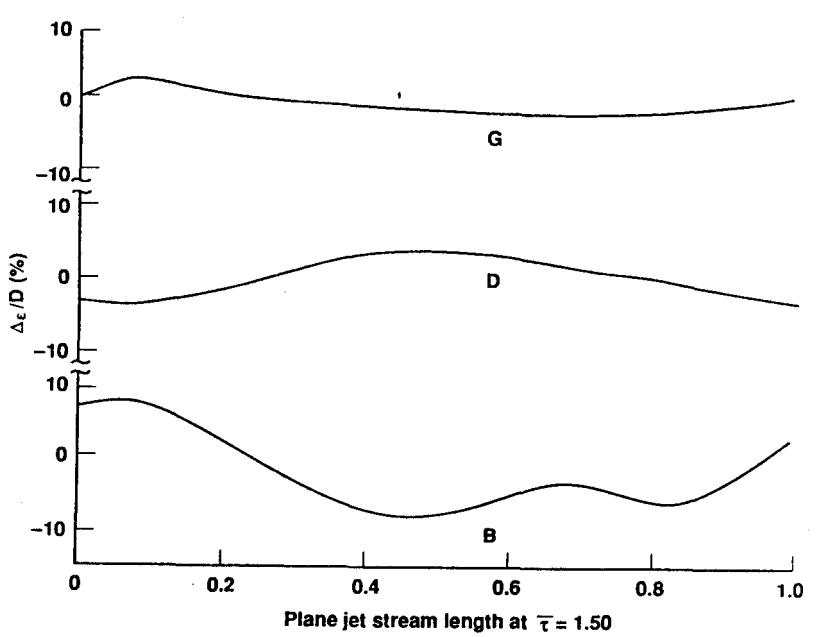

Figure 7. Thin jet fuel sheet deformations at $\bar{\tau} = 1.50$ for three variations in injected jet velocity.

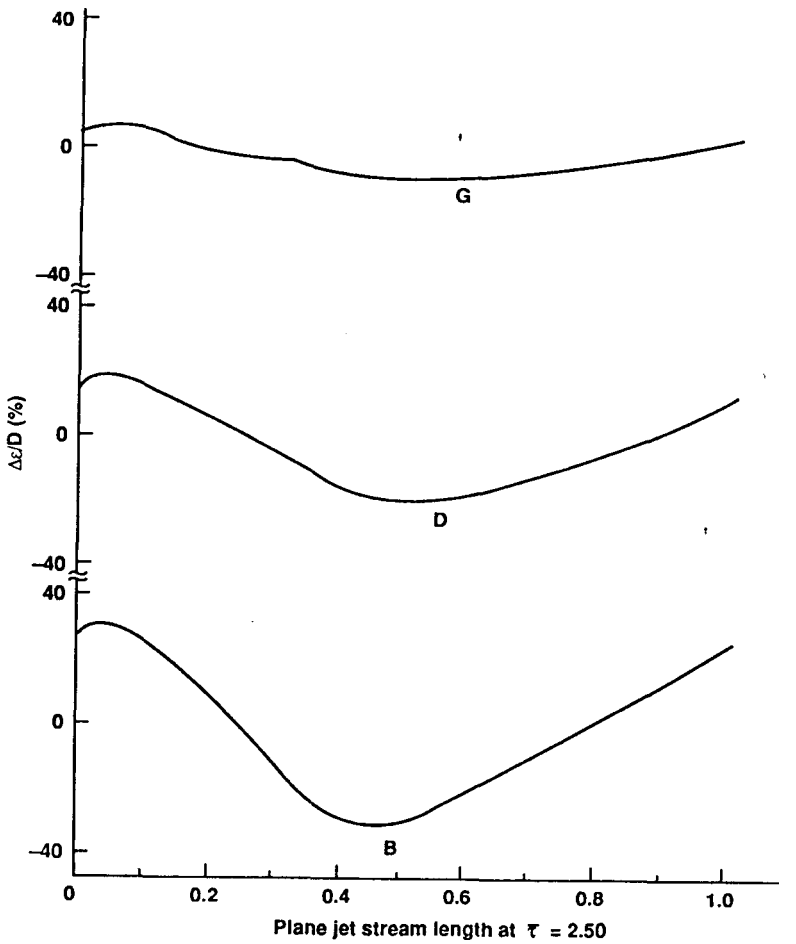

Figure 8. Thin jet fuel sheet deformations at $\bar{\tau}$ = 2.50 for three variations in injected jet velocity.

Effectively, the influence of any leading-edge-density penetration instability is spread among modes more rapidly with higher streamwise advection of the disturbance signal. Penetration instability modes are seen to grow more rapidly at lower values of tangential velocity that advects them.

The opposite trend would be suggested for Kelvin-Helmholtz shearing instabilities. They grow with increasing shear velocity which is directly related to the jet streaming velocity in this geometry. However, with the thin injection sheet geometry and the lack of viscous diffusion of the shear deformation forces, the shearing vortical diffusion is suppressed and the influence is not obvious. Resolution of the competition between shearing instability and leading-edge origin Rayleigh-Taylor instabilities await our later viscous interface simulations, particularly the SHALE results in axial symmetry. Other significant influences such as that of surface tension, which may be significant at least at lower pressures [9,10], will be evaluated separately at the LP gun environmental conditions with the SHALE code axisymmetric simulations.

CONCLUSIONS

- Two-dimensional plane and axially symmetric computer experiments show early promise in complementing and augmenting theoretical analysis and predictions about flow-geometry influences on predicting timing of jet stream breakup, subsequent droplet/clump sizing and, perhaps, dispersal of these fuel jet entities under various chamber pressure, injection velocity, and LP material property value permutations.
- The computer simulations provide a seemingly useful approximation for predicting the influence of the sensitivity of the jet breakup dynamics to the influence of uncertainties in jet-fuel properties at realistically severe (high pressure) LP gun conditions.
- Systematic permutation of the LP fuel-jet injection velocity appears to result in a lessened tendency for LP jet breakup although the influence of shear tearing (Kelvin-Helmholtz) modes and axially symmetric geometry remain to be investigated at later stages.

ACKNOWLEDGMENT

The authors gratefully acknowledge the consistent interest and continuing support for this research from the Department of the Army and the Department of Energy. It is a pleasure to acknowledge also the consultations and assistance of our colleagues at Lawrence Livermore National Laboratory and the Ballistics Research Laboratory. It is a very great pleasure to acknowledge, with thanks, the tireless and very professional efforts of Mrs. J. Noecker in editing, formatting, and timely preparation of the final manuscript and in her excellent and rapid organization of the corrections and rewritten portons despite the awkwardness of coordinating input from the authors' two Laboratories located at opposite sides of the Continent.

REFERENCES

1. Buckingham, A.C., "Compressible Two-Phase Flow Instabilities Simulated with a Hybrid Lagrange-Euler Pseudospectral Method", in *Numerical Methods in Laminar and Turbulent Flow*, **VI**, ed. C.E.T Pineridge Press, Swansea UK (1985), 1427-1438.

2. Buckingham, A.C., "Combustion Instabilities in Liquid Propellants", *Energy & Technology Review*, ed. G.L. Struble, Lawrence Livermore National Laboratory, Livermore CA (1985), 1-8.

3. Bracco, F.V., "High Pressure injection of Liquid Sprays", ARO/BRL/JANNAF Workshop: *Ignition and Combustion of Liquid Monopropellants in a Regenerative Liquid Propellant Gun*, Raleigh NC (Oct 9-10, 1986), 7-12.

4. Youngs, D.L., "Numerical Simulation of Turbulent Mixing by Rayleigh-Taylor Instability", *Physica*, **12D**, North Holland, Amsterdam NL, (1984), 32-44.

5. Read, D.L., "Experimental Investigation of Turbulent Mixing by Rayleigh-Taylor Instability", *Physica*, **12D**, North Holland, Amsterdam NL, (1984), 45-58.

6. Chandrasekhar, S., *Hydrodynamic and Hydromagnetic Stability*, Oxford Univ. Press, UK (1961), Chap. XI.

7. Layzer, D., "On the Instability of Superposed Fluids in a Gravitational Field", *Astrophysical Journ.*, **122** (1), (1955).

8. Plesset, M.S., and Hsieh, D.-Y., "General Analysis on the Stability of Superposed Fluids, *Phys. of Fluids*, **7**, (8), (1964), 1099-1108.

9. Lin, S.P., and Kang, D.J., "Atomization of a Liquid Jet", *Phys. Fluids*, **30**, (7), (1987), 2000-2006.

10. Taylor, G.I., *The Scientific Papers of G.I. Taylor*, Cambridge University Press, UK, (1963), **2**, 25.

11. Demuth, R.G., Margolin, L.G., Nichols, B.D., Adams, T.F., and Smith, B.W., *SHALE: A Computer Program for Solid Dynamics*, Los Alamos National Laboratory Report LA-10236, UC-32 (issued May 1985).

12. Margolin, L.G., Leith, C.E., Tarwater, E., Compton, J., and Beason, C., Discussions and personal communications, recommendations on modifications to SHALE Code for axially symmetric, viscous fluidynamics instability simulations and turbulent mixing. Lawrence Livermore National Laboratory, (1988-1989).